ELSEVIER

Physics of the Earth and Planetary Interiors 117 (2000) 111–121

PHYSICS OF THE EARTH AND PLANETARY INTERIORS

www.elsevier.com/locate/pepi

Control of inner core rotation by electromagnetic, gravitational and mechanical torques

Jonathan Aurnou *, Peter Olson

Department of Earth and Planetary Sciences, Johns Hopkins University, Baltimore, MD 21218 USA

Received 28 October 1998; accepted 20 April 1999

Abstract

We compute the polar rotation of the Earth's inner core in response to the combined effects of electromagnetic, gravitational and mechanical torques. We obtain electromagnetic torques between 10^{18} and 10^{20} Nm, compared to gravitational torques between 10^{19} and 10^{21} Nm estimated by Xu et al. [Xu, S., Crossley D., Szeto, A.M.K., 1999. Variations in length of day and inner core differential rotation from gravitational coupling. Phys. Earth Planet. Inter., 116, 95–110] and Buffett [Buffett, B.A., 1996b. A mechanism for decade fluctuations in the length of day. Geophys. Res. Lett., 23, 3803–3806.], respectively. We obtain mechanical torques on the order of 10^{15} Nm. Gravitationally dominated cases produce inner core oscillations with periods between 1 and 10 years. In electromagnetically dominated cases, the inner core rotates close to the imposed rotation rate of the outer core fluid. Modulations in the rotation rate are produced as the inner core passes through successive gravitational wells. These modulations occur over roughly 90 year timescales for outer core flow rates of 1°/year. When the electromagnetic torques are only marginally stronger than the gravitational torques, the inner core slowly rotates prograde by 90° relative to the mantle, escaping a gravitational well in roughly 100 years, then falls into the next gravitational well, rotating through 90° in just 4 years. Finite inner core viscosity is modeled using a relaxation time for the inner core topography. With relaxation, the gravitational torque reduces but does not eliminate the anomalous inner core rotation. Because of the short timescales of many of the irregularities in inner core rotation, it may be possible to observe them in presently-available seismic data.

Keywords: Inner core rotation; Electromagnetic torques; Gravitational torques; Mechanical torques

1. Introduction

Seismic studies inferring that the Earth's inner core rotates to the east with respect to the mantle have stimulated a broad effort to understand the dynamics of inner core rotation. The dynamo calculations of Glatzmaier and Roberts (1995; 1996) produce a prograde rotation rate of the inner core that scales to a couple of degrees per year. In their calculations, super-rotation can be explained in terms of an electromagnetic couple between the inner and outer core, first proposed by Gubbins (1981). This couple links the rotational motion of the solid inner core to an outer core thermal wind flow located within the tangent cylinder, the imaginary right cylinder that circumscribes the inner core equator (Aurnou et al., 1996, 1998; Glatzmaier and Roberts,

* Corresponding author. Tel.: +1-410-516-7077; fax: +1-410-516-7933; e-mail: aurnou@gibbs.eps.jhu.edu

0031-9201/00/$ - see front matter
PII: S0031-9201(99)00091-6

1996). The dynamo model of Sakuraba and Kono (1998) also features an eastward rotation of the inner core produced by electromagnetic coupling between the inner core and the motion of the adjacent outer core fluid. In their model, the dominant electromagnetic torque on the inner core results from an eastward mean flow just exterior to the inner core tangent cylinder.

Gravitational torques acting between the mantle and the inner core may also serve as a controlling mechanism for inner core rotation. The importance of gravitational torques has been studied by Buffett (1996a; b; 1997) and by Szeto and Xu (1997), and Xu et al. (1999). Buffett (1996a; b) finds that the gravitational torque on the inner core may be on the order of 10^{21} Nm in amplitude. Making different assumptions, Xu et al. (1999) estimate this same gravitational torque to be on the order of 10^{19} Nm. For comparison, the strength of electromagnetic torques on the inner core has been estimated to lie between 10^{16} and 10^{20} Nm (Gubbins, 1981; Glatzmaier and Roberts, 1996; Aurnou et al., 1998). Thus, it is possible that the gravitational and electromagnetic torques on the inner core are comparable in magnitude, and the inner core rotation may depend on a delicate balance between the two.

There are a wide range of seismologically-based estimates of the present-day inner core rotation. Song and Richards (1996) estimated that the inner core rotates eastward with respect to the mantle at $\Omega_{IC} = 1.1^\circ/\text{year}$, based on variations in travel times for seismic rays traveling along polar paths. Another study by Su et al. (1996) made use of travel time data from the ISC catalogue, producing $\Omega_{IC} \simeq 3^\circ/\text{year}$. Creager (1997), using the same data used by Song and Richards (1996) but different modeling assumptions about the inner core anisotropy, found a prograde rotation rate of only $\Omega_{IC} = 0.25^\circ/\text{year}$. Some seismic studies question the existence of an anomalous inner core rotation. It has been argued that the initial $\Omega_{IC} = 3^\circ/\text{year}$ estimate by Su et al. is an artefact of incomplete data coverage (Souriau, 1998; Dziewonski and Su, 1998; Souriau et al., 1997). Souriau (1998) and Souriau et al. (1997) also challenge the findings of Song and Richards (1996), citing possible travel time errors in the data.

In this paper, we use axisymmetric models of the Earth's core to examine possible modes of rotation of the inner core subject to the combined effects of electromagnetic, gravitational and mechanical torques about the polar axis of the inner core. Our calculations show that for strong electromagnetic torques, the inner core spins in the direction of the overlying outer core fluid flow, with superposed periodic perturbations in rotation rate due to the effects of gravity. For strong gravitational torques the inner core oscillates about a fixed orientation relative to the mantle. When the electromagnetic torque is only marginally stronger than the gravitational torque, the rotation of the inner core is still prograde but has a complex history, including steps. The addition of a finite inner core viscosity changes the role of gravitational torques from tending to lock the inner core to retarding its anomalous rotation. According to our calculations, the effects of mechanical torques are relatively small and play a minor role in the inner core rotation.

2. Definition of the model

We assume that the motion of the fluid outer core and the solid inner core both consist of solid body rotation about a common polar axis. Relative to the mantle, the outer and inner core angular velocities are Ω_{OC} and Ω_{IC}, as shown in Fig. 1. We suppose that Ω_{OC} is constant in time, and only Ω_{IC} varies in response to the torques applied to the inner core. When a velocity difference exists across the inner core boundary (ICB), as depicted in Fig. 1, toroidal magnetic fields are induced which produce electromagnetic torques. The existence of a velocity difference across the ICB also leads to an exchange of momentum across the ICB, producing mechanical drag torques. Furthermore, if the shapes of the ICB and the core–mantle boundary (CMB) are triaxial, gravitational torques can be generated between the inner core and the mantle as shown by Buffett (1996a) and Szeto and Xu (1997).

In previous papers on inner core rotation (Aurnou et al., 1996, 1998), we considered the equilibrium between the inner core rotation and toroidal fields generated throughout the whole core. The timescale for the whole system to reach equilibrium was found to be on the order of 30,000 years. In this paper, we focus on the transient response of the inner core to

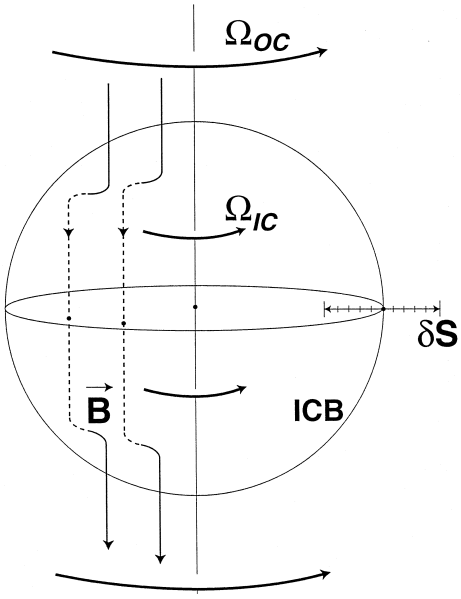

Fig. 1. Schematic showing differential motion between the outer core fluid moving at angular velocity Ω_{OC} and the solid inner core at Ω_{IC}, both relative to the mantle. The magnetic field, $\vec{\mathbf{B}}$, is shown as a solid line in the outer core and as a dashed line inside the inner core. Velocity differences across the inner core boundary (ICB) induce a toroidal magnetic field component, leading to electromagnetic torques on the inner core. This velocity difference also leads to mechanical drag torques on the inner core. The width of the computational shell used in the calculations is shown by the segment $\delta\mathbf{S}$.

perturbations in its rotation rate. Timescales for this process are decades or at most centuries. On this shorter timescale, the only significant magnetic field changes are the toroidal fields induced by the shear across the ICB. We therefore compute the electromagnetic torque on the inner core by assuming that the poloidal field is constant and that the shear-induced field is the only toroidal field.

We model the rotation of the inner core about its polar axis using the following angular momentum balance:

$$I\frac{\mathrm{d}(\Omega_{\mathrm{IC}})}{\mathrm{d}t} = \Gamma_{\mathrm{em}} + \Gamma_{\mathrm{grav}} + \Gamma_{\mathrm{drag}} \tag{1}$$

and

$$\frac{\mathrm{d}\phi}{\mathrm{d}t} = \Omega_{\mathrm{IC}} \tag{2}$$

where ϕ is the azimuthal angular displacement of the inner core. In (1), I is the polar moment of inertia of the inner core (given in Table 1) and the terms on the right hand side are the electromagnetic torque Γ_{em}, the gravitational torque Γ_{grav}, and the torque produced by mechanical drag Γ_{drag}. The combined effects of Γ_{em}, Γ_{grav}, and Γ_{drag} can lead to multiple inner core rotation modes which depend upon the relative strengths of the torques.

First, consider electromagnetic torques on the inner core. The polar component of the electromagnetic torque is given by (Rochester, 1962)

$$\Gamma_{\mathrm{em}} = \frac{1}{\mu_{\mathrm{o}}}\int_{\mathrm{ICB}} B_{\mathrm{r}} B_{\phi}\, r \sin\theta \,\mathrm{d}S \tag{3}$$

where μ_{o} is the magnetic permeability, B_{r} is the radial field on the ICB, B_{ϕ} is the azimuthal field on the ICB and $\mathrm{d}S$ represents a surface element over the ICB which is assumed to be spherical. According to (3), nonzero magnetic fields oriented in the ϕ direction must be present at the ICB for any electromagnetic torques to be generated. These toroidal fields are part of the core dynamo and also are induced by the shear layer formed at the ICB whenever the angular velocity of the inner core, Ω_{IC}, differs from the angular velocity of the outer core fluid, Ω_{OC}.

To calculate the electromagnetic torques, we impose a uniform poloidal magnetic field

$$\vec{\mathbf{B}}_{\mathrm{P}} = -B_{\mathrm{o}}\,\hat{z} \tag{4}$$

where B_{o} is the amplitude in milliTesla (mT) of the magnetic field, so that the components of the poloidal magnetic field on the ICB are $(B_{\mathrm{r}}, B_{\theta}) = -B_{\mathrm{o}}\,(\cos\theta, -\sin\theta)$. The azimuthal field on the ICB, B_{ϕ} in (3), is generated by the interaction of the poloidal magnetic field with the shear layer at the ICB.

The electromagnetic torques tend to minimize the shear across the ICB. When the poloidal field lines crossing the ICB remain unsheared, no electromagnetic torques are exerted. Alternatively, if there is a difference in rotation rate between the inner core and the outer core fluid, Lorentz forces are produced which act to restore the field lines to their initially poloidal state, generating an electromagnetic torque that tends to drive the inner core into co-rotation with the surrounding outer core fluid.

Table 1
Parameter values in numerical calculations and torque estimates

Symbol	Quantity	Value
Ω_{OC}	outer core angular velocity relative to the mantle	0.25–3.0°/yr*
I	inner core polar moment of inertia	5.87×10^{34} kg m^2
R_I	inner core radius	1.22×10^{6} m
R_{CMB}	outer core radius	3.48×10^{6} m
B_o	polidal magnetic field intensity	0.37–1.07 mT*
μ	magnetic permeability	$4\pi\times10^{-7}$ H m^{-1}
η	magnetic diffusivity	2.65 m^2/s*
ν	outer core kinematic viscosity	10^{-7} m^2/s*
ρ	fluid density at ICB	1.25×10^{4} kg/m^3

*Assumed values.

Mechanical stresses also occur at the ICB whenever Ω_{IC} is not equal to Ω_{OC}. The mechanical drag torque directed along the polar axis of the inner core is given by

$$\Gamma_{drag} = \hat{z}\cdot\int_{ICB}\vec{r}\times\vec{\tau}\,dS \tag{5}$$

where $\vec{\tau}$ is the shear stress exerted on an ICB surface element. We consider separately two sources of mechanical drag: viscous stress and turbulent stress. The laminar viscous stress on the inner core is $\vec{\tau}=\rho\nu[(\partial u_\phi/\partial r)-(u_\phi/r)]\hat{e}_\phi$ where ρ is the density of the fluid at the ICB, υ is the kinematic viscosity of the fluid (see Table 1), u_ϕ is the azimuthal velocity and $\hat{e}_\phi$ is a unit vector in the ϕ-direction. In the ICB shear layer, the u_ϕ/r term in the viscous stress is small and we neglect it. Substituting the viscous stress into (5) yields the torque due to azimuthal, laminar viscous flow:

$$\Gamma_{visc} = \int_{ICB} s\left(\rho\nu\frac{\partial u_\phi}{\partial r}\right)dS \tag{6}$$

where $s=r\sin\theta$ is the cylindrical radius. In order of magnitude, this torque is approximately $\Gamma_{visc}\sim\rho\nu\Omega_{IC}R_I^4/\delta_{bl}\sim10^{13}$ Nm, where we use the inner core radius R_I to scale s, and $R_I\Omega_{IC}/\delta_{bl}$ to scale du_ϕ/dr. Here, we assume the Ekman boundary layer thickness δ_{bl} to be on the order of 50 cm and we use $\Omega_{IC}=1°$/year in all the scaling arguments.

However, the assumption that mechanical drag is controlled by laminar viscous stresses may not be justifiable. Using the values given in Table 1, we estimate the Reynolds number for the fluid flow around the inner core to be $Re\sim\Omega_{IC}R_I^2/\nu\sim10^9$. For such a large value of Re, it is expected that the boundary layer at the ICB will be turbulent. Therefore, we expect the most significant mechanical torque on the inner core is due to the turbulence in the boundary layer. In this situation, a quadratic drag law similar to those used for the atmospheric boundary layer or the benthic boundary layer in the ocean provides an estimate of this torque (Gill, 1982; Stull, 1988; Garratt, 1992). A standard quadratic mechanical drag law is (Gill, 1982)

$$\vec{\tau}=\rho C_D|\vec{u}|\vec{u} \tag{7}$$

where $\vec{u}$ is the fluid velocity in the free stream outside the boundary layer and C_D is the empirically-derived, nondimensional drag coefficient that is on the order of 10^{-3} in a broad range of geophysical situations (Gill, 1982; Garratt, 1992). Substituting (7) into (5) and integrating over the surface of the inner core gives the turbulent mechanical drag torque:

$$\Gamma_{turb} = \int_{ICB} s\left(\rho C_D s^2[\Omega_{OC}-\Omega_{IC}]^2\right)dS \tag{8}$$

$$\simeq \frac{3\pi^2}{4}\rho C_D\Omega_{IC}^2R_I^5 \tag{9}$$

$$\sim 10^{15}\ \text{Nm} \tag{10}$$

This estimate of Γ_{turb} does not take into account the turning that the flow will undergo in the Ekman layer surrounding the inner core (Garratt, 1992). Even so, Γ_{turb} greatly exceeds Γ_{visc} at the ICB. We therefore neglect the torque due to laminar viscous drag and include only the contribution of turbulence to the mechanical drag torque on the inner core.

Fig. 2 is a sketch of the Earth's core showing how axial gravitational torques can be generated on the inner core. In this figure the shape of the CMB is perturbed into an triaxial ellipsoid. This CMB deformation results from dynamical stresses due to flow in the convecting mantle. Large-scale downwellings in the lower mantle will depress the CMB while regions of upwelling mantle flow will tend to elevate the CMB. Here, we assume the inner core has a

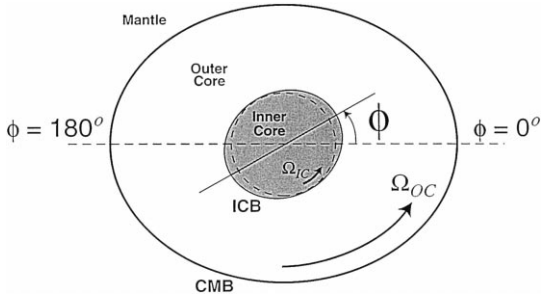

Fig. 2. Equatorial plan view of the Earth's core showing the assumed triaxiality of the ICB and core–mantle boundary (CMB). The triaxiality of the ICB and the CMB are greatly exaggerated in this figure. Gravitational torques tend to restore the inner core to the equilibrium locations $\phi = 0°$, 180°. Adapted from Buffett (1996a).

given triaxial shape and that this triaxiality is constant in time. We also take the rotation axis of the inner core to be parallel to the rotation axis of the mantle. This corresponds to the case of zero inner core obliquity angle in the calculations of Szeto and Xu (1997), and Xu et al. (1999). The ellipticity of the inner core equator is estimated to be on the order of 10^{-4} and we do not account for this ellipticity in the electromagnetic torque Eq. (3).

The axial gravitational torque is found at first order to be (Xu et al., 1999)

$$\Gamma_{\rm grav}(\phi) = -\Gamma_{\rm g} \sin 2\phi \qquad (11)$$

where ϕ is the angular displacement of the inner core from the gravitational equilibrium position shown in Fig. 2. The coefficient $\Gamma_{\rm g}$ represents the maximum gravitational torque imparted to the inner core, occurring whenever ϕ has a value equal to an integer multiple of 45°. This gravitational torque acts to restore the inner core to the nearest gravitational equilibrium position, situated at either $\phi = 0°$ or 180°.

If we include only gravitational torques and perturb the inner core a small angular distance away from $\phi = 0°$, then the angular momentum balance (1) can be rewritten as

$$\frac{{\rm d}^2\phi}{{\rm d}t^2} + \omega_{\rm g}^2\phi = 0 \ \text{ where } \ \omega_{\rm g} = \sqrt{\frac{2\Gamma_{\rm g}}{I}} \qquad (12)$$

Here, we have substituted ${\rm d}^2\phi/{\rm d}t^2$ for ${\rm d}\Omega_{\rm IC}/{\rm d}t$. Eq. (12) describes a simple harmonic oscillator with natural frequency $\omega_{\rm g}$. Using the value of I in Table 1, the period of gravitational oscillations of the inner core is $2\pi/\omega_{\rm g} = 10.8$ years for Xu et al.'s torque (Xu et al., 1999) $\Gamma_{\rm g} = 10^{19}$ Nm and $2\pi/\omega_{\rm g} = 1.08$ years for Buffett's torque (Buffett, 1996b) $\Gamma_{\rm g} = 10^{21}$ Nm.

3. Numerical model for the combined torques

In order to calculate the electromagnetic torque in (3), the induced azimuthal magnetic field B_ϕ is determined using the induction equation:

$$\left(\frac{\partial}{\partial t} - \eta\left(\nabla^2 - \frac{1}{s^2}\right)\right) B_\phi = B_{\rm r}\frac{\partial u_\phi}{\partial r} + \frac{B_\theta}{r}\frac{\partial u_\phi}{\partial \theta} \qquad (13)$$

where η is the magnetic diffusivity, $s = r\sin\theta$ is the cylindrical radius, $(B_{\rm r},\ B_\theta)$ are defined by (4) and the azimuthal velocity is defined as

$$u_\phi = \begin{cases} s\,\Omega_{\rm IC} & \text{for} \quad r \le R_{\rm I} \\ s\,\Omega_{\rm OC} & \text{for} \quad r > R_{\rm I} \end{cases} \qquad (14)$$

such that velocity gradients exist only across the ICB. We assume axisymmetry and use the 50×50 ''shell'' grid in $(r,\ \theta)$ that is described by Aurnou et al. (1998). The computational shell is centered around the ICB and has a thickness $\delta\mathbf{S}$ that is $1/10$ the radius of the CMB (see Fig. 1). The resulting radial nodal spacing is $\Delta r = 7$ km. A 25-h time step is used based on the magnetic diffusion time for the shell. The boundary conditions for solving (13) are

$$B_\phi = 0 \ \text{ at } \ \theta = 0, \pi \qquad (15)$$

$$B_\phi = 0 \ \text{ at } \ r = R_{\rm I} \pm 1/2\,\delta\mathbf{S} \qquad (16)$$

The first condition (15) assures that the toroidal field vanishes along the rotation axis and the second condition (16) forces the toroidal field to zero at $R_{\rm I} \pm 1/2\delta\mathbf{S}$, the edges of the computational shell. Because the toroidal field is induced at the ICB and decays quickly with distance (Aurnou et al., 1998), we find that forcing this field to zero at the edges of the computational shell (16), instead of at $r = 0$ and $R_{\rm CMB}$, does not noticeably affect our solutions.

The tangential electric field must remain continuous across the ICB which produces a jump condition in the azimuthal magnetic field at the ICB. In these

calculations, as in the work Aurnou et al. (1998), we directly integrate the induction equation across the ICB, producing an error in our solutions that is on the order of $\Delta r/R_{\mathrm{CMB}}$. This error is less than 1% in all of our calculations.

The calculations are all initialized with $\Omega_{\mathrm{IC}} = 0$ at $t = 0$. In the cases without gravitational torques, the value of the inner core angular displacement is initially set to $\phi_{\mathrm{i}} = 0°$. When gravitational torques are present, the angular displacement is initialized to $\phi_{\mathrm{i}} = 10°$ in order to perturb the inner core from the bottom of the gravitational well located at $\phi = 0°$.

The computational scheme utilizes second-order finite differences in space and explicit, first-order time stepping in solving (1), (2), (3), (8), (11) and (13) subject to conditions (15) and (16). We calculate the electromagnetic torque (3) with the magnetic field values from the previous time step, the mechanical torque (8) with the angular velocity values from the previous time step and the gravitational torque (11) with the value of ϕ from the previous time step. These torques are used in (1) to compute Ω_{IC} in the present time step. The value of Ω_{IC} from the previous time step is used to calculate the azimuthal magnetic induction in (13) subject to (15) and (16).

4. Response to individual torques

4.1. Electromagnetic torques

Fig. 3 shows the angular displacement of the inner core relative to the mantle vs. time assuming only electromagnetic torque, for two different poloidal magnetic field strengths. The flow in the outer core fluid is imposed at $\Omega_{\mathrm{OC}} = 1°/\mathrm{year}$ and the amplitude of the imposed poloidal field is $B_{\mathrm{o}} =$ 0.37 mT (solid line) and $B_{\mathrm{o}} = 1.07$ mT (dashed line). The lower poloidal field value of 0.37 mT is estimated by downward continuation to the poles of the CMB of the axial dipole Gauss coefficient from the International Geomagnetic Reference Field model, $g_1^0 \cong 30{,}000$ nT, assuming that the mantle is an insulator (IAGA Division V, Working Group 8, 1996). The second estimate $B_{\mathrm{o}} = 1.07$ mT is the strength of the poloidal field at the poles of the ICB if we further assume that the poloidal field corresponds to that of a fundamental mode dipole inside the core (Aurnou et al., 1998).

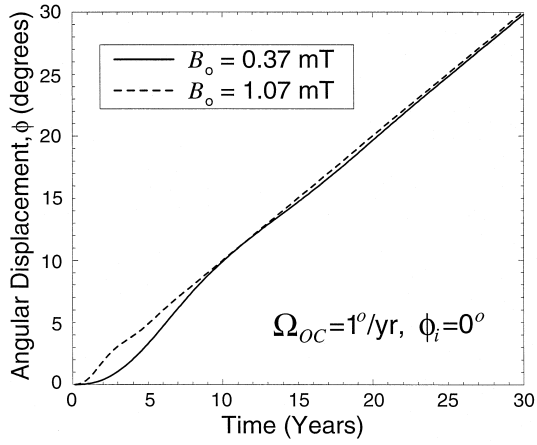

Fig. 3. Inner core angular displacement vs. time due to electromagnetic torques. The electromagnetic torques are generated by a $\Omega_{\mathrm{OC}} = 1°/\mathrm{year}$ outer core fluid flow interacting with a 0.37-mT poloidal field (solid line) and 1.07-mT poloidal field (dashed line).

The electromagnetic torques strongly couple the motion of the inner core to that of the neighboring outer core fluid and the inner core rotates very close to 30° in 30 years. Electromagnetic torques act to drive the inner core eastward such that $\Omega_{\mathrm{IC}} \rightarrow \Omega_{\mathrm{OC}}$. Simultaneously, the electromagnetic torques damp high frequency oscillations in the inner core motion. The coupling between the inner core and the outer core increases with increasing magnetic field strength. This can be seen by the longer oscillation frequency and spin-up time for the $B_{\mathrm{o}} = 0.37$ mT case compared to the $B_{\mathrm{o}} = 1.07$ mT case. The amplitude of the electromagnetic driving torques generated by various outer core flow rates and magnetic field strengths are given in Table 2. These values range from $O(10^{18})$ to $O(10^{20})$ Nm.

4.2. Gravitational torques

In the gravitational torque formula (11) the coefficient Γ_{g} is poorly constrained. Models by Buffett (1996a; b) based on tomographic estimates of lower mantle density anomalies indicate that $\Gamma_{\mathrm{g}} \simeq 10^{21}$ Nm. The models of Szeto and Xu (1997), and Xu et al. (1999) are all based on estimates of the flattening of the CMB and the ICB from geodetic considera-

Table 2
Maximum electromagnetic driving torques

Ω_{OC} [°/yr]	B_o [mT]	Amplitude [Nm]
0.25	0.37	2.58×10^{18}
0.25	1.07	2.18×10^{19}
1.0	0.37	1.03×10^{19}
1.0	1.07	8.58×10^{19}
3.0	0.37	3.09×10^{19}
3.0	1.07	2.57×10^{20}

tions. They estimate that the equatorial flattening of the inner core may be proportional to the second power of the equatorial flattening of the Earth's surface. From this line of reasoning, Szeto and Xu (1997) arrived at an estimate for Γ_g of 10^{19} Nm.

In order to explore the whole range of possible inner core behavior, we take Buffett's estimate of Γ_g as an upper bound and Xu et al.'s estimate as a lower bound. In the cases shown in Fig. 4, the inner core is released from rest with an initial angular displacement of $\phi_i = 10°$ relative to the gravitational potential well located at $\phi = 0°$. The perturbed inner core oscillates around the gravitational equilibrium position with a 10.8 year period for $\Gamma_g = 10^{19}$ Nm (solid line). For $\Gamma_g = 10^{21}$ Nm, an oscillation period of 1.08 years is found (dashed line). These numerical results precisely agree with the oscillation periods obtained analytically using (12).

4.3. Torque due to mechanical drag of the outer core fluid

Fig. 5 shows the inner core angular displacement vs. time due to the turbulent mechanical drag torques for $\Omega_{OC} = 1°/\text{year}$ (solid line) and $\Omega_{OC} = 3°/\text{year}$ (dashed line). Even though the mechanical drag torque on the inner core due to turbulent friction scales to roughly 2–3 orders of magnitude greater than the torque due to laminar viscous drag, the mechanical drag torque is still four orders of magnitude smaller than the electromagnetic or gravitational torques. After 50 years, $\Omega_{IC} \simeq 0.004°/\text{year}$ when the imposed outer core flow is $1°/\text{year}$ and $\Omega_{IC} \simeq 0.036°/\text{year}$ when the outer core flow is $3°/\text{year}$. Thus, the effects of mechanical drag are insignificant in comparison with the other two torques on the inner core.

Bills (1999) argues that the inner core rotation is affected by flow in the outer core induced by tidal spin-down of the mantle. In our models, similar mechanical torques do not control the rotation of the inner core when electromagnetic or gravitational torques are included.

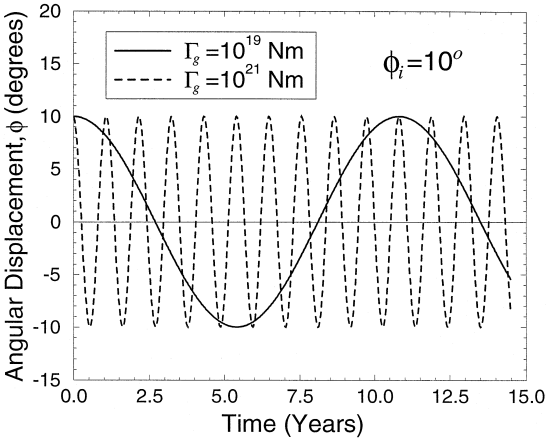

Fig. 4. Inner core angular displacement vs. time due to gravitational torques. The inner core, initially at $\phi_i = 10°$, oscillates within the gravitational well located at $\phi = 0°$. The oscillation period is 10.8 years for $\Gamma_g = 10^{19}$ Nm and 1.08 years for $\Gamma_g = 10^{21}$ Nm.

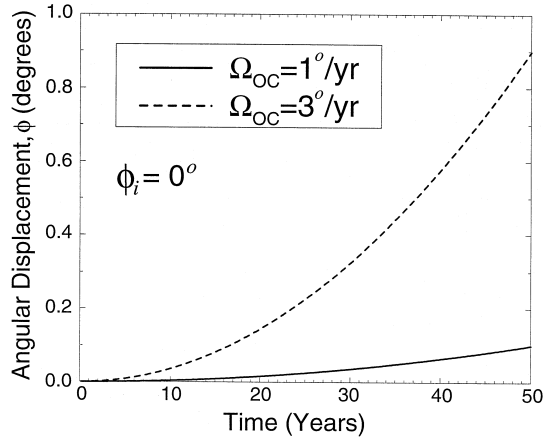

Fig. 5. Inner core angular displacement vs. time due to mechanical drag torques produced by outer core flows of $\Omega_{OC} = 1°/\text{year}$ (solid line) and $\Omega_{OC} = 3°/\text{year}$ (dashed line). The mechanical drag weakly accelerates the inner core into prograde rotation following the prograde flow of the outer core fluid.

5. Combined electromagnetic, mechanical and gravitational torques

In this section, we show the results of computations in which electromagnetic, gravitational and mechanical torques simultaneously act on the inner core. Three types of solutions are found: the gravitationally dominated case, the electromagnetically dominated case and the case where the electromagnetic torques are comparable to the gravitational torques. In the gravitationally dominated case, the perturbed inner core executes underdamped oscillations inside the gravity well of the mantle. When the electromagnetic torque is dominant the inner core rotates at a rate close to that of the fluid outer core with small sinusoidal perturbations in rotation rate due to the effects of the gravitational torques. In the third case, the inner core slowly rotates eastward out of one gravity well (where $\Gamma_{\mathrm{grav}} < 0$) and then falls quickly into the next gravity well (where $\Gamma_{\mathrm{grav}} > 0$). This motion leads to a form of inner core super-rotation with staircase-like steps in ϕ as a function of time.

5.1. Dominant gravitational torques

Fig. 6 shows the angular displacement of the inner core as a function of time for the case of dominant gravitational torques. In this case, the initial value of the inner core angular displacement is $\phi_{\mathrm{i}} = 10°$ and the value of the gravitational torque is $\Gamma_{\mathrm{g}} = 10^{21}$ Nm. The magnetic field strength defined in (4) is $B_{\mathrm{o}} = 1.07$ mT and the flow rate of the outer core fluid is set at $\Omega_{\mathrm{OC}} = 3°/\mathrm{year}$. This combination of parameters produces a peak electromagnetic torque of 2.57×10^{20} Nm.

As shown in Fig. 6, the oscillation period of the inner core is found to be 1.03 years. The oscillations decrease in amplitude with an exponential decay time of roughly 12 years. The inner core oscillates because of the strong gravitational restoring torque and the damping is provided by the velocity-dependent electromagnetic torque. It can be seen in Fig. 6 that the inner core orientation approaches a static equilibrium with $\phi \simeq 2°$. This occurs because the electromagnetic torque, which is nearly $1/4$ the strength of the maximum gravitational torque, acts to drive the inner core out from the bottom of the gravitational well. Thus, in the case where gravitational torques are dominant, these calculations show that any inner core rotational motion will consist of magnetically damped oscillations, which decay toward an equilibrium inner core position located a few degrees eastward of $\phi = 0°$.

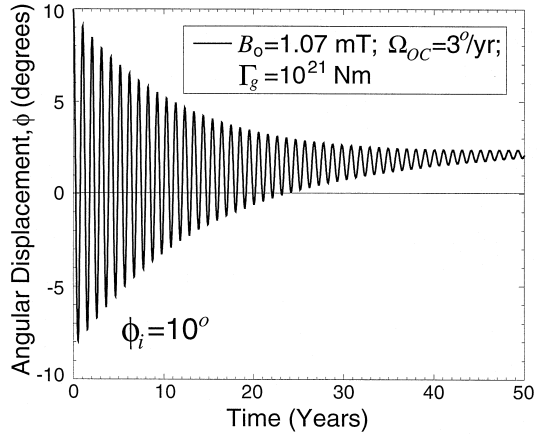

Fig. 6. Inner core angular displacement vs. time due to the interaction of electromagnetic and dominant gravitational torques. The amplitude of the gravitational torque is $\Gamma_{\mathrm{g}} = 10^{21}$ Nm and the maximum amplitude of the electromagnetic torque that drives the inner core to the east is 2.57×10^{20} Nm. The inner core, initially perturbed to $\phi_{\mathrm{i}} = 10°$, oscillates with a 1.03-year period within the gravitational well of the mantle.

5.2. Dominant electromagnetic torques

Fig. 7 shows the angular displacement of the inner core over roughly 300 years with the initial angular displacement $\phi_{\mathrm{i}} = 10°$. A gravitational torque $\Gamma_{\mathrm{g}} = 10^{19}$ Nm is used in these calculations. Four cases are plotted in Fig. 7, all with peak electromagnetic torques that are greater than 10^{19} Nm. Three of the four cases plotted in Fig. 7 (cases b, c and d) escape the gravitational well located at $\phi = 0°$ within the 300 years. In case b, the inner core slowly climbs out of the $\phi = 0°$ gravitational well from $\phi = 10°$ to $\phi = 45°$. Then the inner core sharply accelerates from $\phi = 45°$ to $\phi = 180°$, undergoes damped magnetic oscillations, and slowly climbs out of the gravitational well centered at $\phi = 180°$. The inner core rotations shown in cases c and d are qualitatively

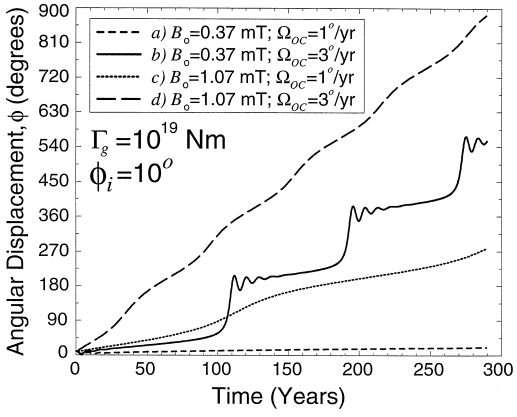

Fig. 7. Inner core angular displacement vs. time due to the interaction of dominant electromagnetic and gravitational torques. The amplitude of the gravitational torque is $\Gamma_g = 10^{19}$ Nm and the peak amplitude of the eastward electromagnetic driving torque in the four cases plotted range from 1.03×10^{19} to 2.57×10^{20} Nm. The initial inner core angular displacement is $\phi_i = 10°$ in the four cases shown.

different from b. These higher magnetic field strength cases exhibit a quasi-linear increase in $\phi(t)$ superimposed upon smooth broad modulations. The modulations are symmetric about the two gravitational wells located at $\phi = 0°$ and 180°.

In the weak field cases (a and b) the maximum electromagnetic torque driving the inner core to the east is stronger than the maximum gravitational torque. In case a, the peak electromagnetic driving torque is only 3% stronger than the gravitational torque. After roughly 900 years, the inner core escapes from the gravity well centered at $\phi = 0°$ and falls rapidly into the well located at $\phi = 180°$. There it undergoes damped oscillations and begins to rotate slowly eastward again.

The peak electromagnetic torque driving the inner core eastward in case b is almost three times the maximal gravitational torque. From $\phi = 0$–45°, the inner core has an average velocity of 0.4°/year. In the region $\phi = 45$–90°, the inner core accelerates out of the $\phi = 0°$ gravity well, and from $\phi = 90°$ to $\phi = 180°$, the inner core falls into the next gravitational well centered at $\phi = 180°$. A maximum rotation rate of 27.6°/year is reached when the inner core is between $\phi = 90$ and 180°. The inner core goes into a magnetically damped oscillation that has a period of roughly 9 years as it nears the bottom of the gravity well at $\phi = 180°$. This cycle then repeats itself as the inner core starts to rotate eastward at a rotation rate of 0.4°/year out of the well located at $\phi = 180°$, eventually falling into the initial gravitational well at $\phi = 360°$. The average velocity of the inner core rotation over a 360° cycle is 1.88°/year. Thus, the rotational motions in cases a and b are qualitatively similar, each showing a strong increase in rotation rate between $\phi = 90°$ and 180°. The difference between the cases is that the dwell time in each successive gravity well is about 16 times greater in case a than in case b.

In the strong field simulations (c and d) the inner core is tightly coupled to the motion of the surrounding outer core fluid and the average value of Ω_{IC} is very close to Ω_{OC}. The broad modulations in angular displacement are due to the inner core moving into and out of successive gravitational wells. The inner core does not over-shoot the equilibrium position of the gravitational wells because the electromagnetic torque strongly damps the inner core motion, maintaining Ω_{IC} close to Ω_{OC}. Since the inner core is rotating at $\Omega_{IC} \sim \Omega_{OC}$, we can recast (11) as $\Omega_{grav} = -\Gamma_g \sin 2\Omega_{OC} t$. The modulations in the inner core rotation will have a period of about 180 years for $\Omega_{OC} = 1°$/year and 60 years for $\Omega_{OC} = 3°$/year. Thus, the temporal frequency of the modulations is controlled by the value of Ω_{OC}, while the amplitude of the modulations decreases with increasing B_0^2 in these cases.

In a case with $\Omega_{OC} = 0.25°$/year and $B_o = 1.07$ mT, the inner core rotation is a mixture of the behaviors shown in cases a, b and cases c, d. Here, the inner core rotates eastward at close to 0.09°/year, escaping the gravitational well at $\phi = 0°$ after about 580 years. The rotation rate increases as it falls into the next well, reaching $\phi = 180°$ after 795 years. The average rotation rate from $\phi = 90°$ to $\phi = 180°$ is close to 0.42°/year, with a peak rotation rate of 0.82°/year occurring at $\phi = 112.5°$. The electromagnetic driving torques are relatively weak in this case so that the rotational motion is asymmetric with respect to the gravitational well locations, similar to cases a and b. On the other hand, with $B_o = 1.07$ mT, the electromagnetic damping is still strong so that the peak inner core rotation rate is always less

than 1°/year and ϕ increases monotonically in time, as in cases c and d.

5.3. Relaxing inner core topography

We have made computations in which the inner core topography is allowed to viscously relax towards the nearest gravitational well. The relaxation occurs as an exponential decay of the displacement angle of the inner core topography with an e-folding time of the relaxation denoted by τ, similar to that of Buffett (1997). In these computations, the inner core topography is tracked by a new variable ϕ_2, the semi-major axis of the inner core topography. To calculate the gravitational torque in this case, ϕ_2 replaces ϕ in (11). The value of ϕ_2 is computed according to

$$\frac{\mathrm{d}\phi_2}{\mathrm{d}t} = \Omega_{\mathrm{IC}} - \frac{(\phi_2 - \phi^*)}{\tau} \tag{17}$$

where $\phi_2 - \phi^*$ is the angle between ϕ_2 and the bottom of the nearest gravitational well.

In Fig. 8, two cases with relaxing inner core topography are shown. The electromagnetic and gravitational torques correspond to those shown in Fig. 6, where the rigid inner core remains locked within the initial gravity well: $\Omega_g = 10^{21}$ Nm, $B_o = 1.07$ mT and $\Omega_{\mathrm{OC}} = 3^\circ$/year. In case a (solid line), the characteristic relaxation time is $\tau = 1$ year. The initial oscillations decay in about 10 years, leaving a steady motion of the inner core at a rotation rate $\Omega_{\mathrm{IC}} = 1.84^\circ$/year, roughly 2/3 of the outer core flow rate. Case b has $\tau = 100$ years (dashed line) and is similar to the case of a rigid inner core shown in Fig. 6. At longer times, case b differs from the rigid case: the rigid case of Fig. 6 remains permanently locked within the gravity well of the mantle for all times, whereas with relaxation the inner core continues to rotate in the prograde direction. After 200 years the rotation asymptotes to $\Omega_{\mathrm{IC}} = 0.05^\circ$/year. These computations show that gravitational torques have only secondary effects on the inner core rotation when the inner core relaxation time $\tau < 5$ years, while the inner core rotation is similar to the rigid cases for $\tau > 50$ years.

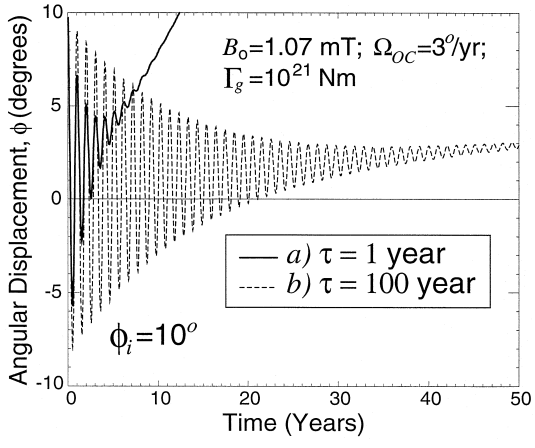

Fig. 8. Inner core angular displacement vs. time due to the interaction of electromagnetic torques and gravitational torques, including viscous relaxation of the inner core topography. In case a, the characteristic relaxation time is $\tau = 1$ year and in case b, $\tau = 100$ years. The amplitude of the gravitational torque is $\Gamma_g = 10^{21}$ Nm and the maximum amplitude of the electromagnetic torque that drives the inner core to the east is 2.57×10^{20} Nm. Note that the inner core does not remain locked within the initial gravitational well in cases with relaxing inner core topography.

6. Conclusions

We have modeled the polar rotational motions of a triaxial inner core subject to the combined action of electromagnetic, gravitational and mechanical torques. The stretching of the poloidal magnetic field lines by shearing at the ICB acts to couple the rotational motion of the inner core to the motion of the adjacent outer core fluid. By imposing an eastward flow of the outer core fluid, electromagnetic torques with amplitudes between 10^{18} and 10^{20} Nm drive the inner core into super-rotation such that the rotation rate of the inner core approaches that of the outer core. Gravitational torques, caused by the interaction between the gravitational field of the mantle and topography on the ICB, couple the inner core to the mantle. These torques are estimated to be between 10^{19} and 10^{21} Nm. Mechanical drag due to the turbulent boundary layer at the ICB produces torques on the order of 10^{15} Nm. The mechanical drag torque is of secondary importance compared to the gravitational and electromagnetic torques.

Depending on the relative strengths of the electromagnetic and gravitational torques, several inner core

rotational modes are possible. In the cases where the electromagnetic torque is weaker than the gravitational torque, the inner core rotation consists of damped oscillations in the gravitational well of the mantle. When the electromagnetic torque is much greater than the gravitational torque, the inner core rotates at an average rate equal to that of the surrounding outer core fluid. The rotation rate of the inner core oscillates around the outer core fluid angular velocity as the inner core passes in and out of mantle gravitational wells. In the cases where the electromagnetic torques are only slightly greater than the gravitational torques, the inner core slowly climbs out of one gravitational well and then rapidly falls into the next. This stepping motion has two very distinct rotation rates, a slow motion of less than $1^\circ/$year, and a fast motion of nearly $30^\circ/$year. Relaxation of the inner core topography changes the effect of the gravitational torque from locking to retarding the inner core, resulting in a broader range of parameters over which the inner core is found to super-rotate.

The results presented here show that the timescales of possible inner core rotational modes are well within the 30-year window of available seismic data and could also be observable in geodetic measurements of Earth's rotation. The period of the gravitational oscillations varies from 1 to 10 years for gravitational torques between 10^{19} and 10^{21} Nm, respectively. Modulations in the inner core rotation rate occur on a timescale of roughly 90 years for $\Omega_{OC} = 1^\circ/$year and 30 years for $\Omega_{OC} = 3^\circ/$year, in cases where the electromagnetic torques dominate over the gravitational torques. When the electromagnetic torques are only slightly greater than the gravitational torques, the inner core is found to rotate from $\phi = 90^\circ$ to $\phi = 180^\circ$ on a timescale of roughly 4 years, followed by damped 9-year oscillations.

References

Aurnou, J.M., Brito, D., Olson, P.L., 1996. Mechanics of inner core super-rotation. Geophys. Res. Lett. 23, 3401–3404.

Aurnou, J.M., Brito, D., Olson, P.L., 1998. Anomalous rotation of the inner core and the toroidal magnetic field. J. Geophys. Res. 103, 9721–9738.

Bills, B.G., 1999. Tidal despinning of the mantle, inner core superrotation and outer core effective viscosity. J. Geophys. Res. 104, 2653–2666.

Buffett, B.A., 1996a. Gravitational oscillations in the length of day. Geophys. Res. Lett. 23, 2279–2282.

Buffett, B.A., 1996b. A mechanism for decade fluctuations in the length of day. Geophys. Res. Lett. 23, 3803–3806.

Buffett, B.A., 1997. Geodynamic estimates of the viscosity of the Earth's inner core. Nature 388, 571–573.

Creager, K.C., 1997. Inner core rotation from small-scale heterogeneity and time-varying travel times. Science 278, 1284–1288.

Dziewonski, A.M., Su, W.J., 1998. A local anomaly in the inner core. EOS Trans. Am. Geophys. Union 79 (17), S218.

Garratt, J.R., 1992. The Atmospheric Boundary Layer. Cambridge Univ. Press, Cambridge, p. 316.

Gill, A.E., 1982. Atmosphere–Ocean Dynamics. Academic Press, San Diego, p. 662.

Glatzmaier, G.A., Roberts, P.H., 1995. A three-dimensional convective dynamo solution with rotating and finitely conducting inner core and mantle. Phys. Earth Planet. Inter. 91, 63–75.

Glatzmaier, G.A., Roberts, P.H., 1996. Rotation and magnetism of Earth's inner core. Science 274, 1887–1891.

Gubbins, D., 1981. Rotation of the inner core. J. Geophys. Res. 86, 11695–11699.

IAGA Division V, Working Group 8, 1996. EOS Trans. Am. Geophys. Union 77, 153.

Rochester, M.G., 1962. Geomagnetic core–mantle coupling. J. Geophys. Res. 67, 4833–4836.

Sakuraba, A., Kono, M., 1998. Effects of the inner core on the numerical solution of the magnetohydrodynamic dynamo. Phys. Earth Planet. Inter. 111, 105–121.

Song, X., Richards, P.G., 1996. Observational evidence for differential rotation of the Earth's inner core. Nature 382, 221–224.

Souriau, A., 1998. Earth's inner core: Is the rotation real?. Science 281, 55–56.

Souriau, A., Roudil, P., Moynot, B., 1997. Inner core differential rotation: facts and artefacts. Geophys. Res. Lett. 24, 2103–2106.

Stull, R.B., 1988. An Introduction to Boundary Layer Meteorology. Kluwer Academic Publishers, Netherlands, p. 666.

Su, W.J., Dziewonski, A.M., Jeanloz, R., 1996. Planet within a planet: rotation of the inner core of the Earth. Science 274, 1883–1887.

Szeto, A.M.K., Xu, S., 1997. Gravitational coupling in a triaxial ellipsoidal shell. J. Geophys. Res. 102, 27651–27657.

Xu, S., Crossley, D., Szeto, A.M.K., 1999. Variations in length of day and inner core differential rotation from gravitational coupling. Phys. Earth Planet. Inter. 116, 95–110.